Supplementary Information (SI) for New Journal of Chemistry.

Supplementary Information

Facile Synthesis of Nickel and Cobalt Oxide integrated 3-D Porous Nitrogen-Doped Carbon derived from *Psidium guajava* (PNDC/$NiCo_2O_4$) for supercapacitor application

Gaurav Mukherjee[a], Asha Raveendran[a], Chuanxiang Chen[b], Masoom Raza Siddiqui[c], Saikh Mohammad Wabaidur[c], Ragupathy Dhanusuraman[a,d]*

[a]*Nano Electrochemistry Lab (NEL), Department of Chemistry, National Institute of Technology Puducherry, Karaikal - 609609, India*

[b]*School of Environmental and Chemical Engineering, Jiangsu University of Science and Technology, 212100 Zhenjiang, China*

[c]*Chemistry Department, College of Science, King Saud University, Riyadh 11451, Saudi Arabia*

[a,d] *Nano Electrochemistry Laboratory (NEL), Central Instrumentation Facility (CIF), School of Physical, Chemical and Applied Sciences, Pondicherry University, Puducherry - 605014, India*

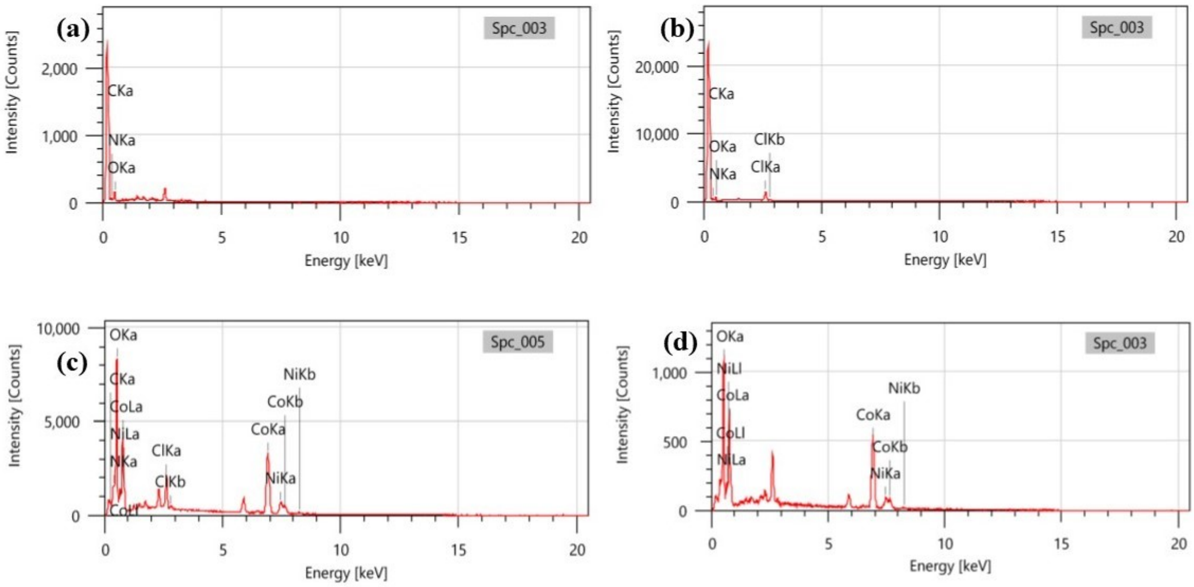

Figure S1: EDAX spectra of (a)AC-CO_3,(b) AC-Cl, (c) AC-ClMO, (d) MO

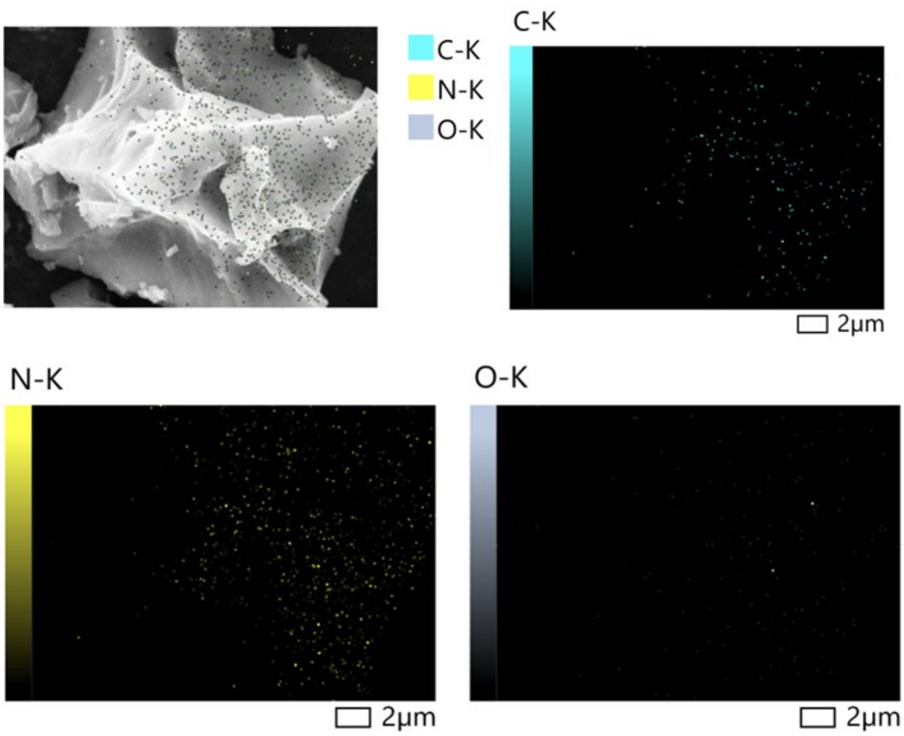

Figure S2: Elemental mapping of AC-CO_3

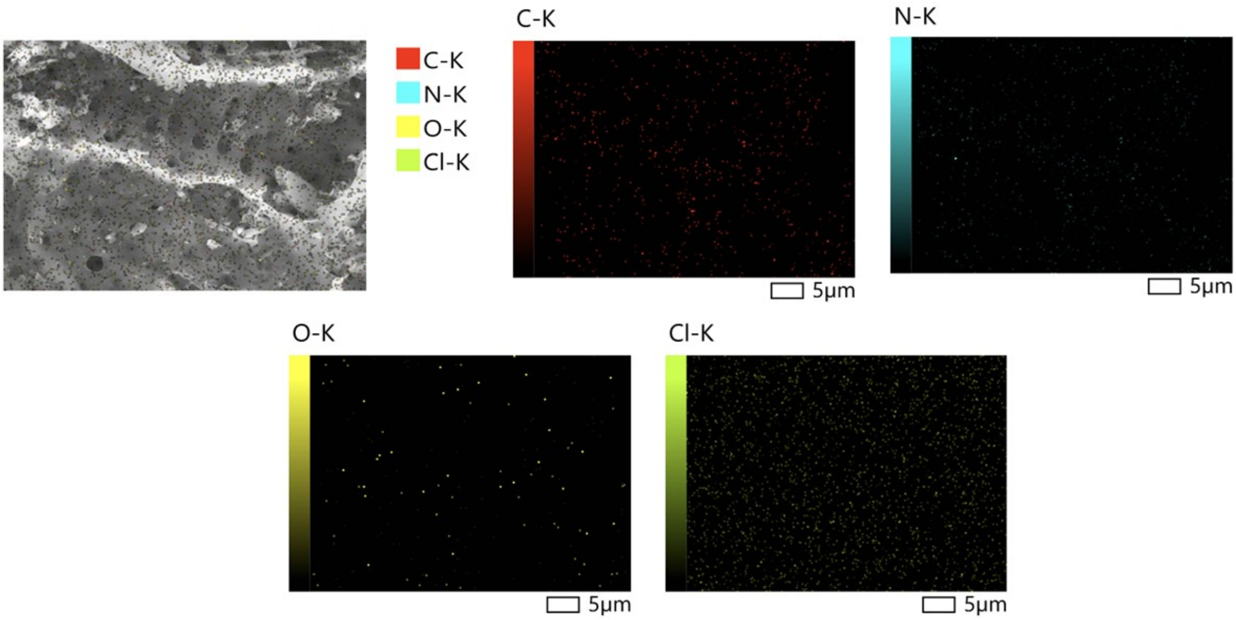

Figure S3: Elemental mapping of AC-Cl

Figure S4: Elemental mapping of AC-ClMO

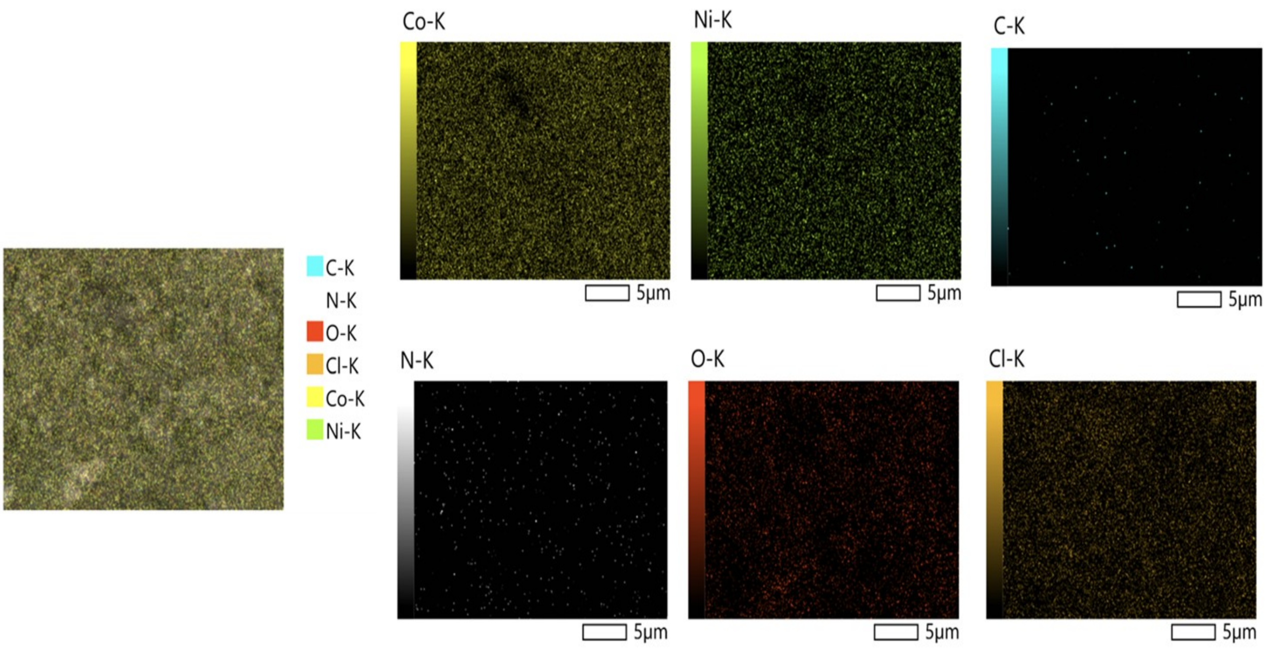

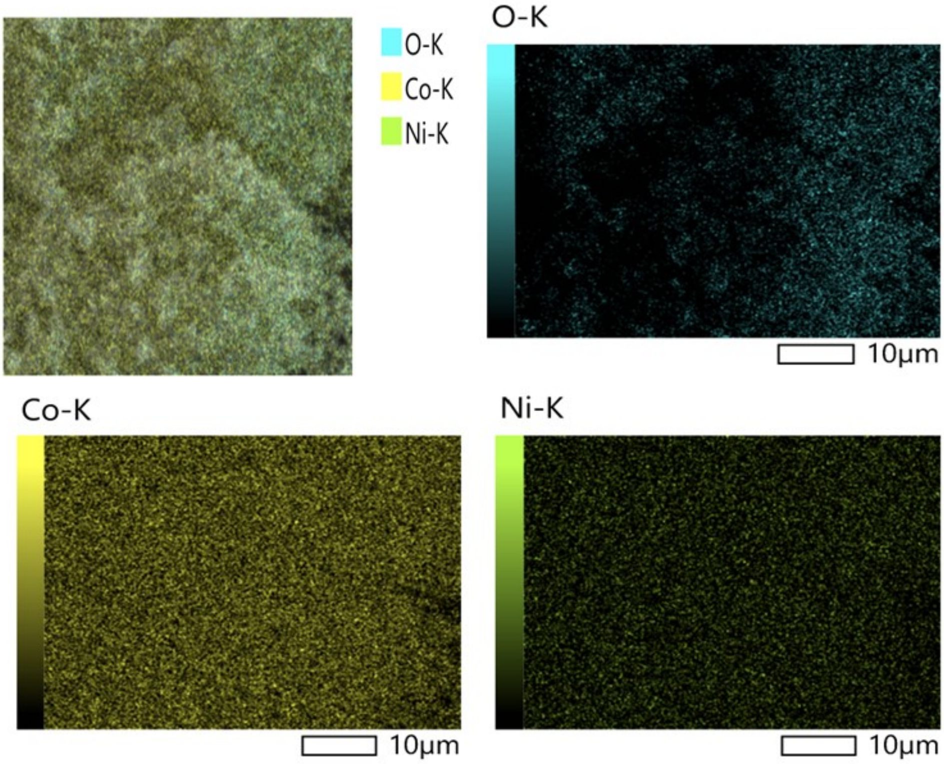

Figure S5: Elemental mapping of MO

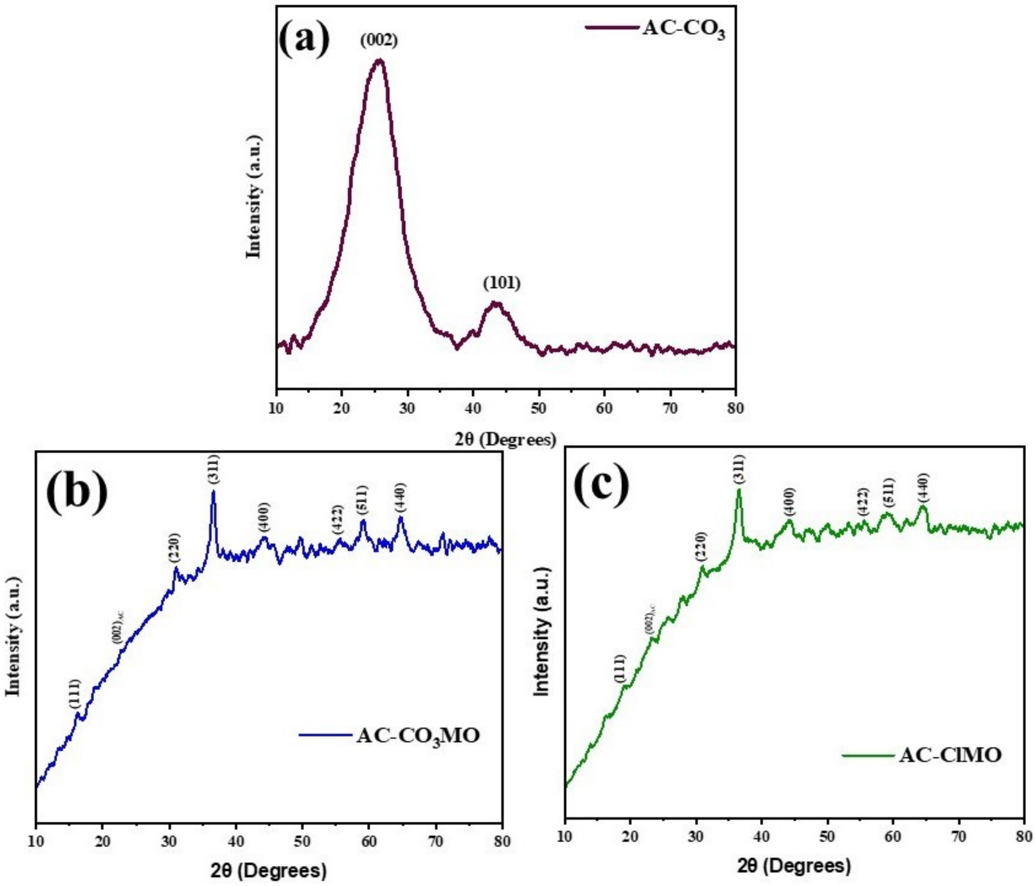

Figure S6: XRD Spectra of: (a) $AC\text{-}CO_3$; (b) $AC\text{-}CO_3MO$; (c) AC-ClMO

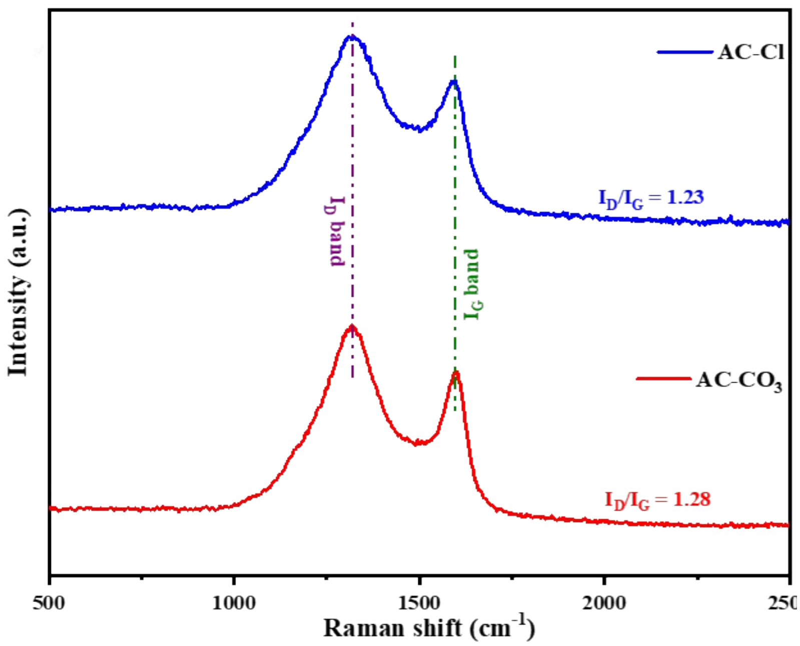

Figure S7: Raman Spectra of Nitrogen-Doped Biochar ($AC\text{-}CO_3$ and AC-Cl)

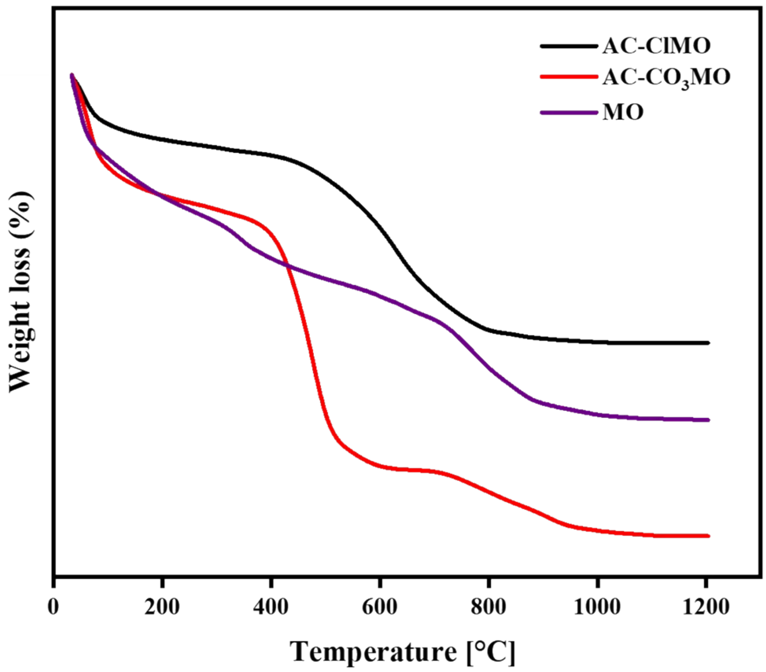

Figure S8: TGA curves of AC-CO_3MO ,AC-ClMO and MO

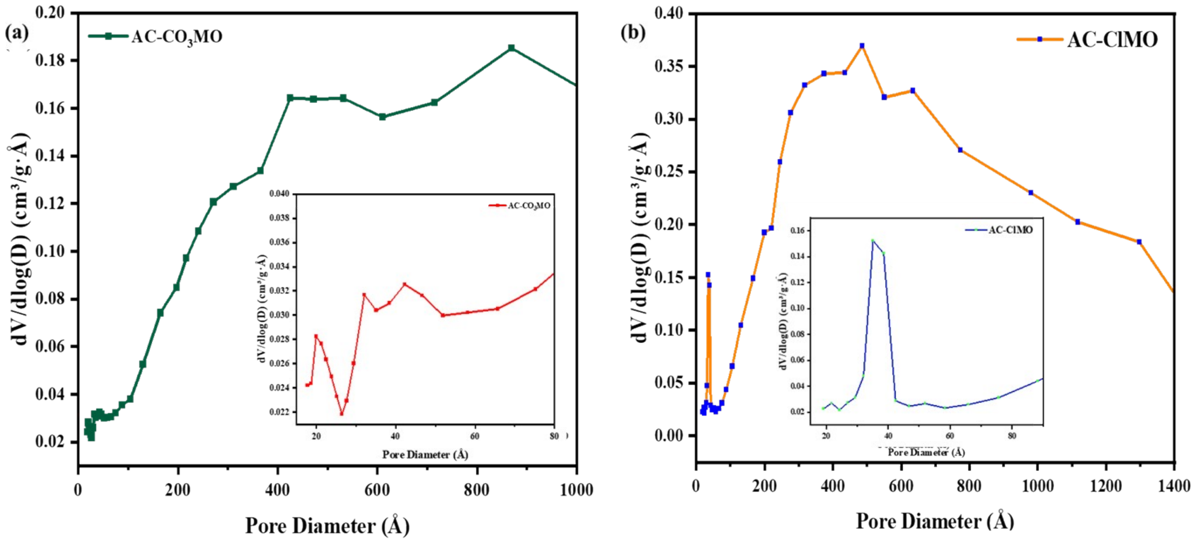

Figure S9: BJH plot: pore size distribution plot for (inset showing magnified view) (a) AC-CO_3MO, (b) AC-ClMO

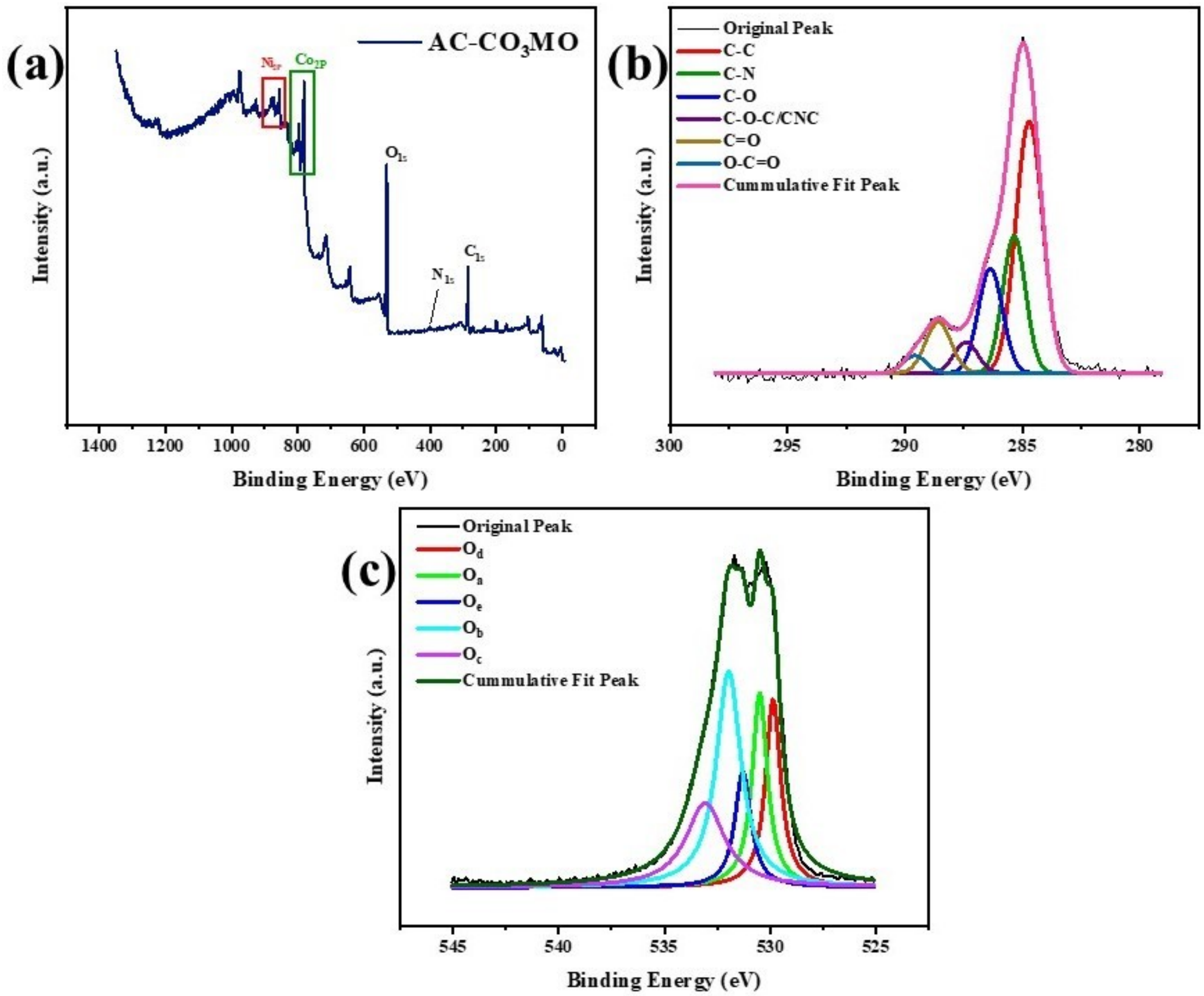

Figure S10 *:* XPS (a) survey and spectra of AC-CO_3MO ((b)C_{1s} core level, (b) O_{1s} core level

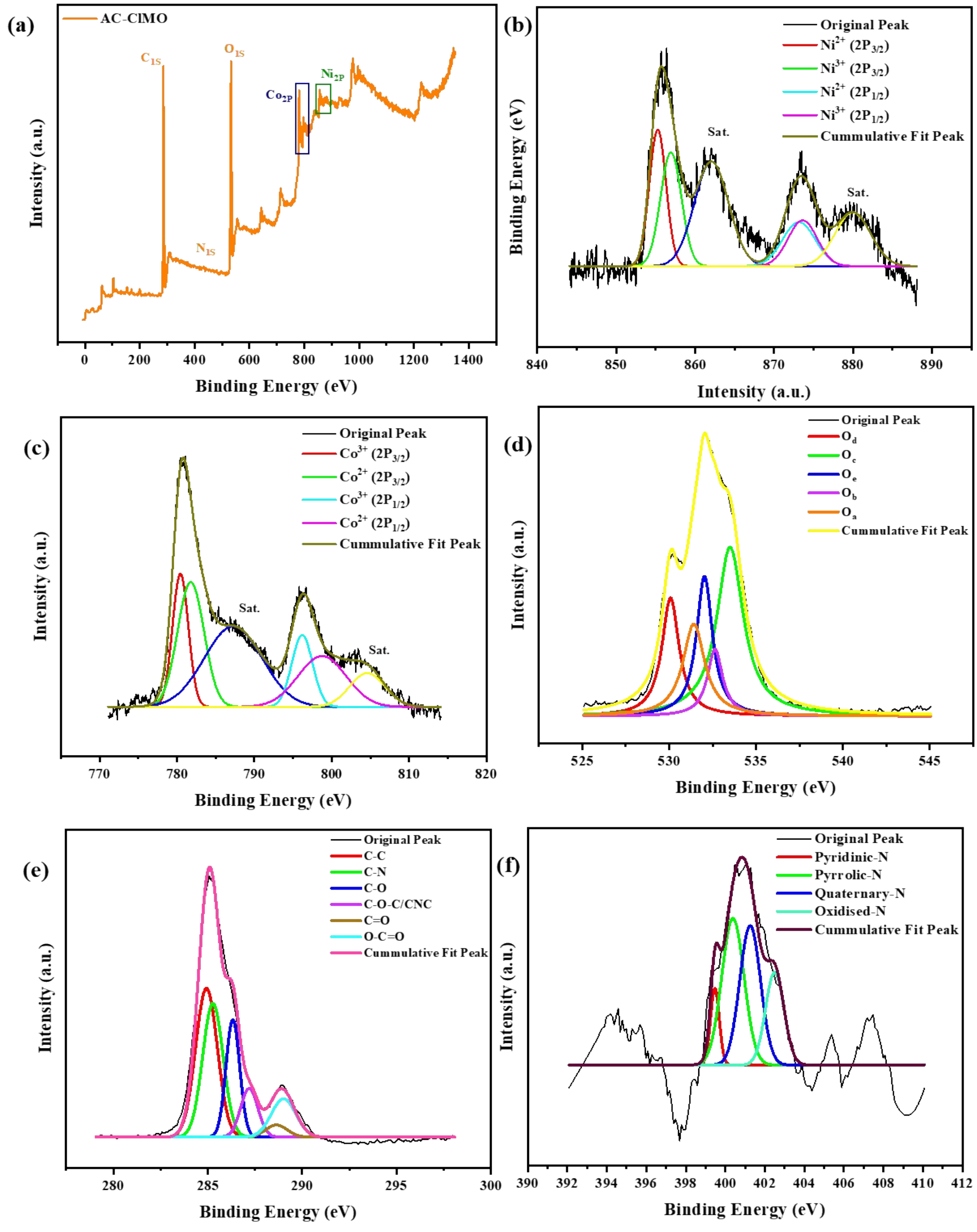

Figure S11 : XPS (a) survey and spectra of AC-ClMO (b) Ni_{2p} core level, (c) Co_{2p} core level (d)C_{1s} core level, (e) O_{1s} core level (f) N_{1s} core level

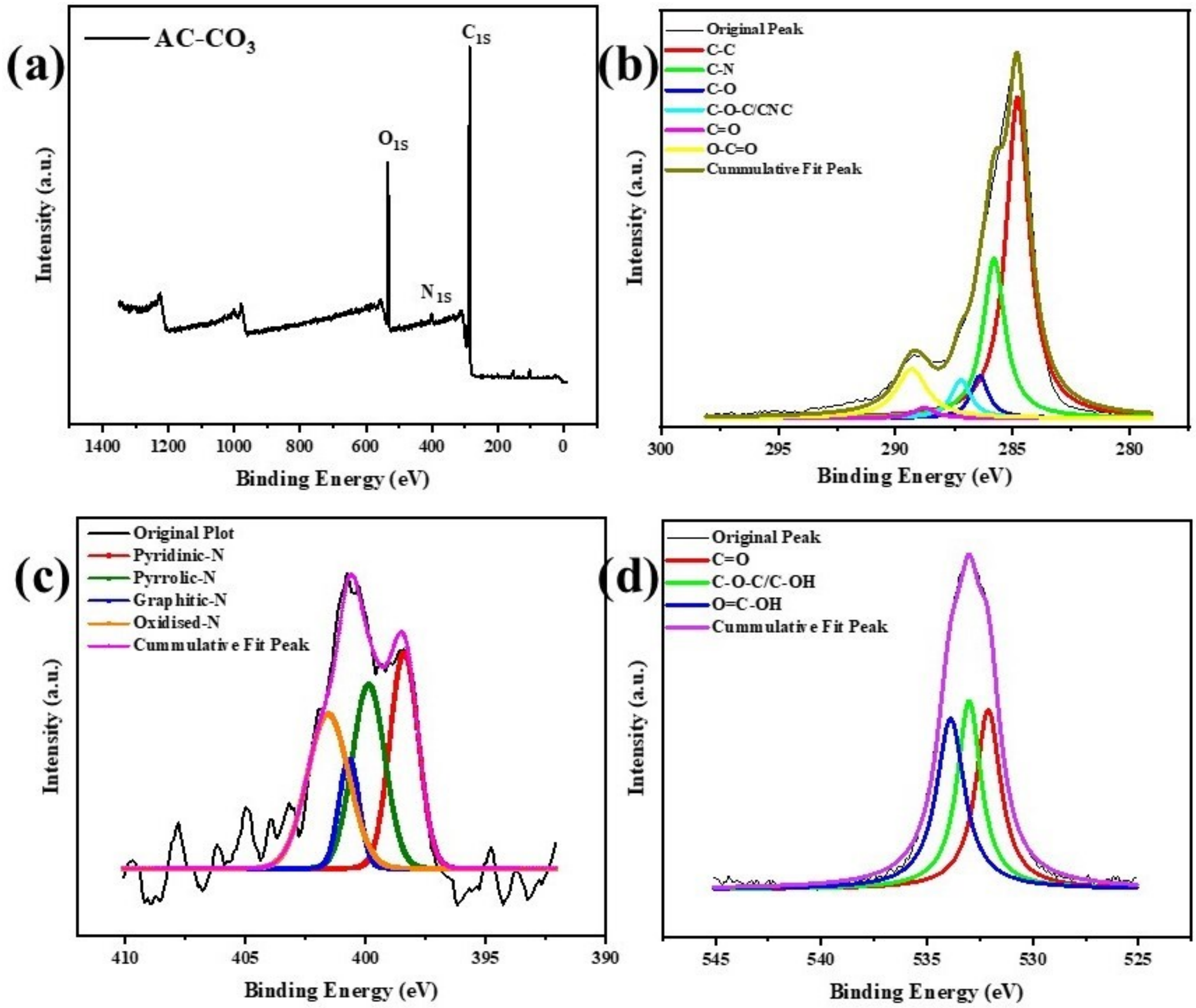

Figure S12 : XPS (a) survey and spectra of $AC\text{-}CO_3$ (b)C_{1s} core level (c) N_{1s} core level (d) O_{1s} core level

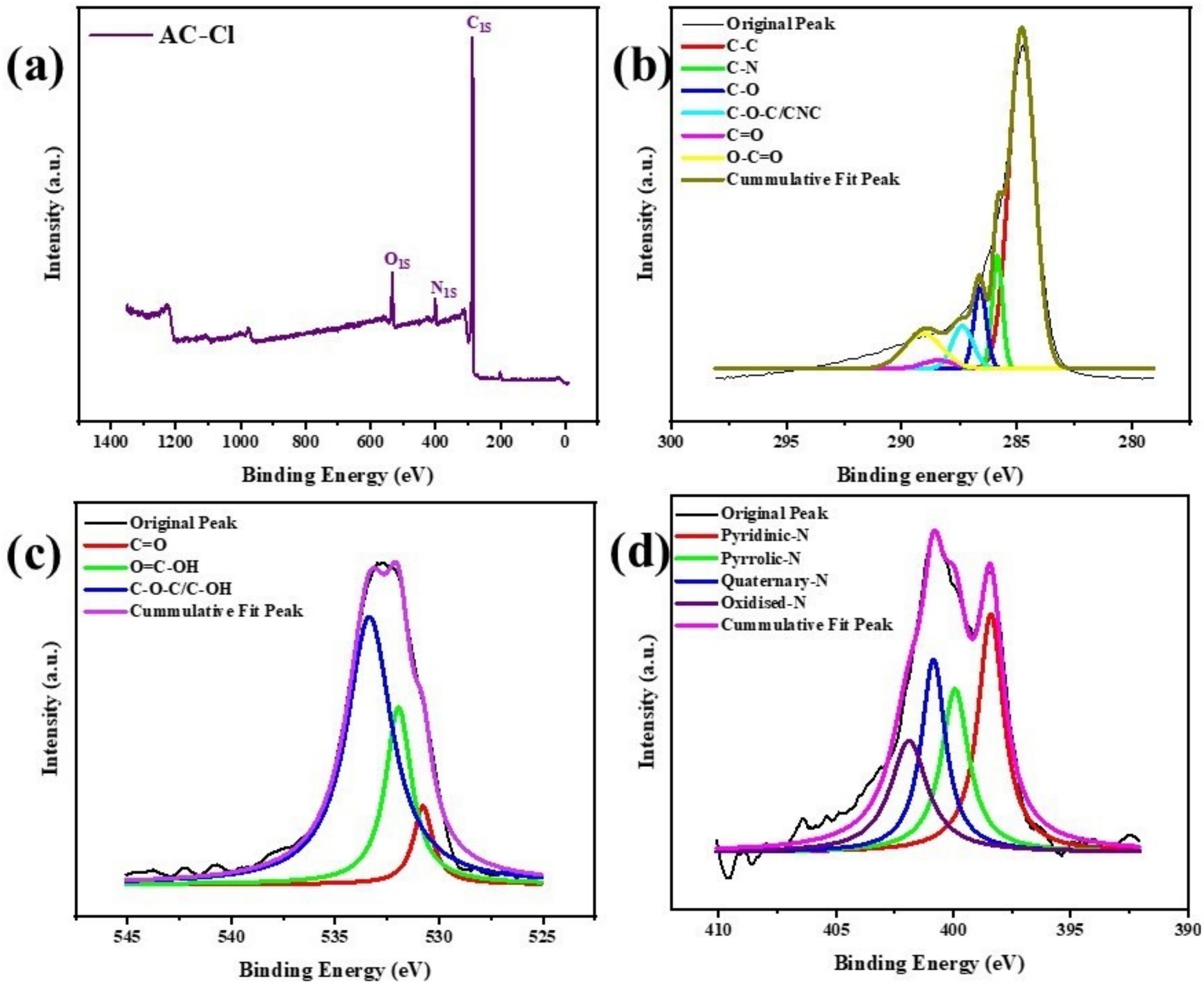

Figure S13 : XPS (a) survey and spectra of AC-Cl (b)C_{1s} core level (c) N_{1s} core level (d) O_{1s} core level

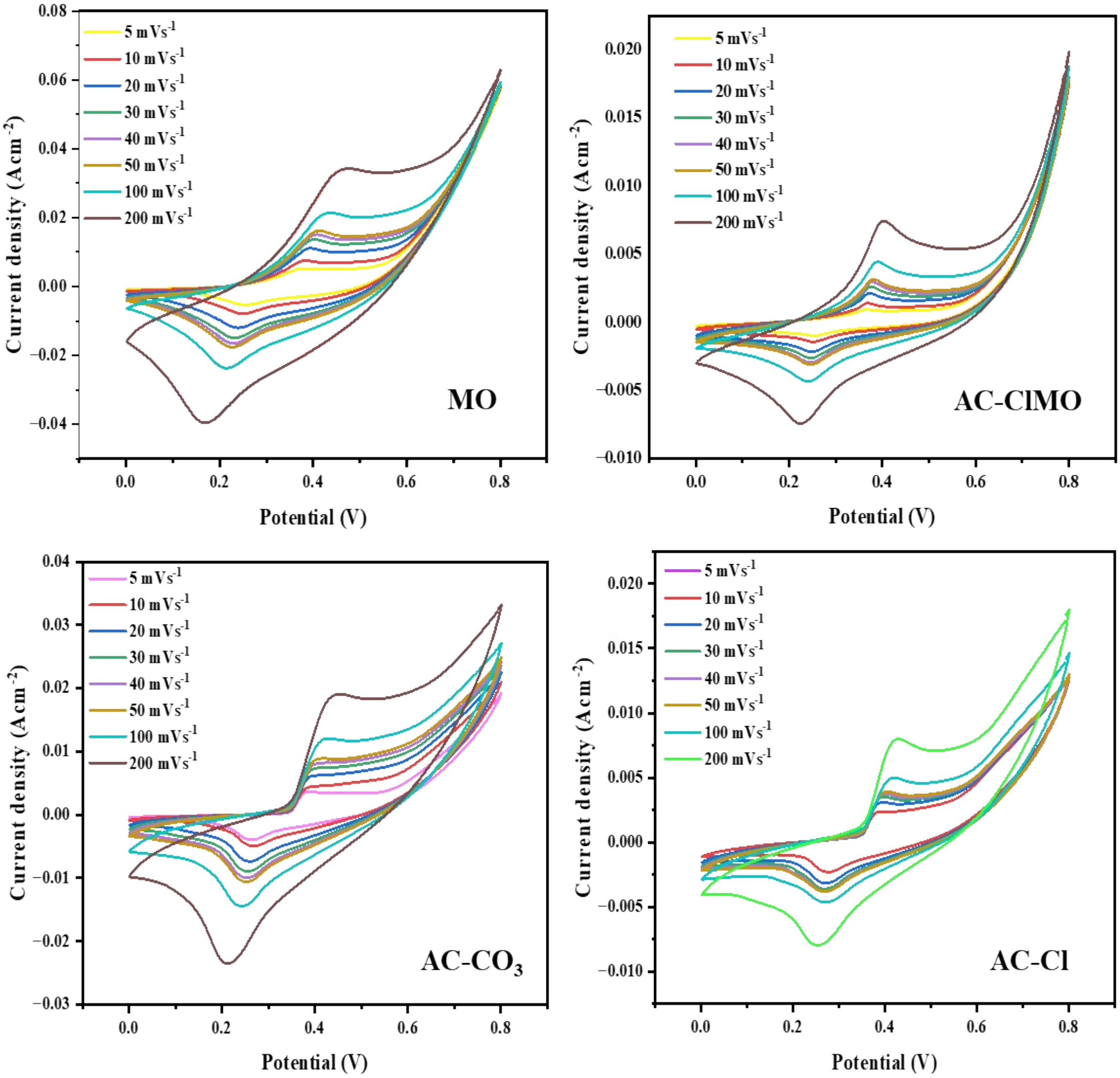

Figure S14: Cyclic voltammogram of (a) MO, (b) AC-ClMO, (c) AC-CO_3, (d) AC-Cl at varying scan rates

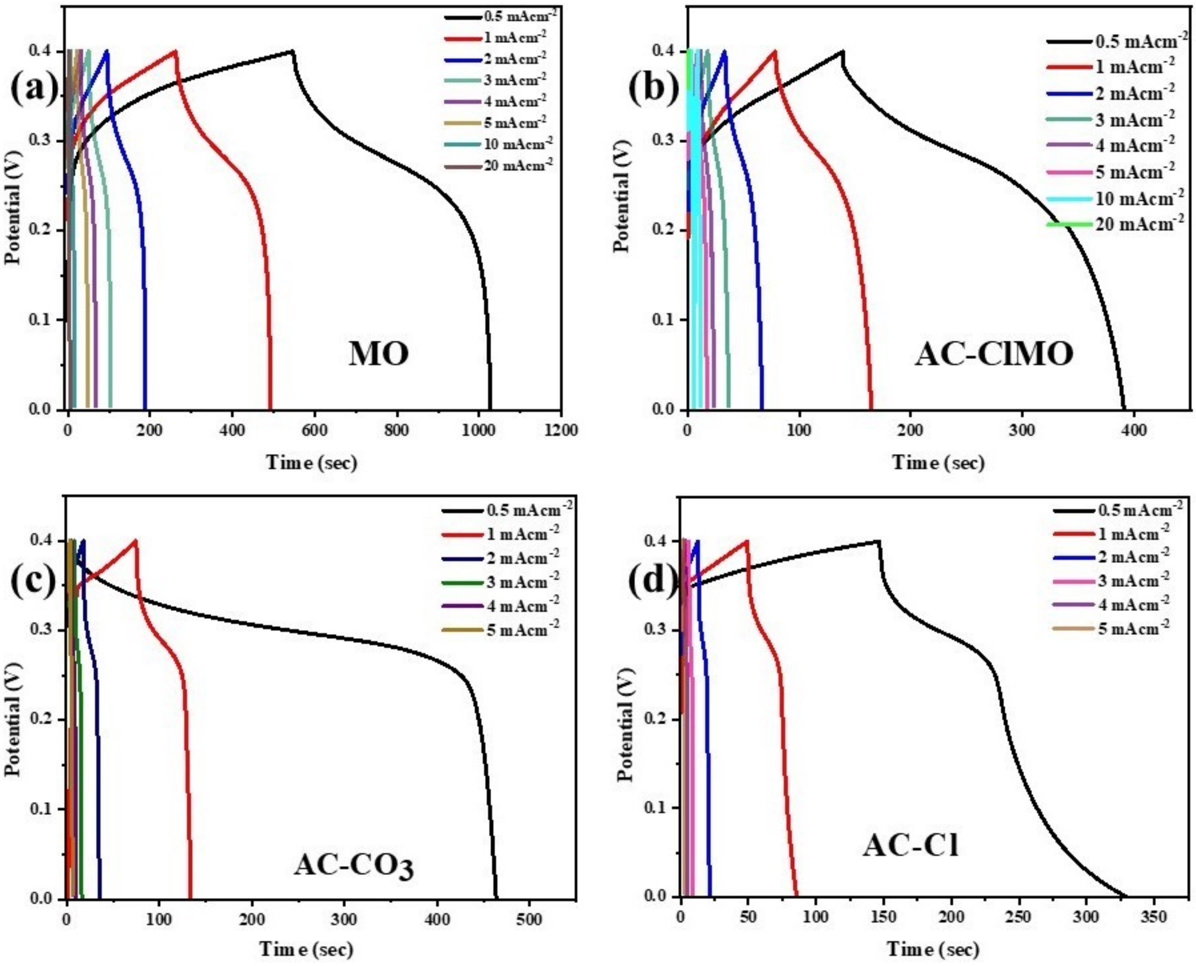

Figure S15: Galvanostatic charge-discharge curves of (a) MO, (b) AC-ClMO, (c) AC-CO_3, (d) AC-Cl at varying scan rates

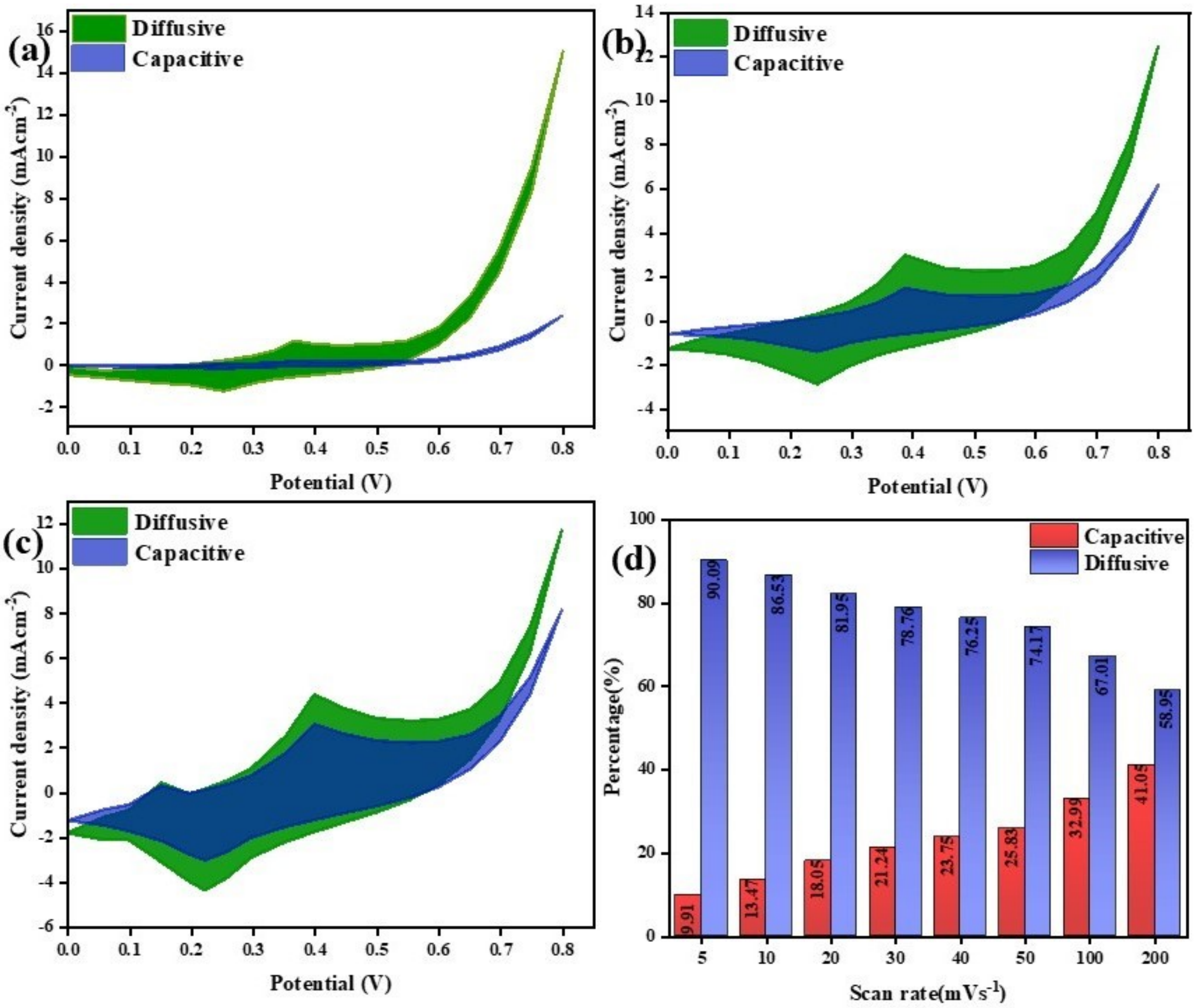

Figure S16: Capacitive and diffusive controlled CV curves of AC-ClMO at scan rates (a) 10mVs^{-1}; (b) 100 mVs^{-1}; (c) 200 mVs^{-1}; and (d) contribution percentage graph at different scan rates of AC-ClMO.

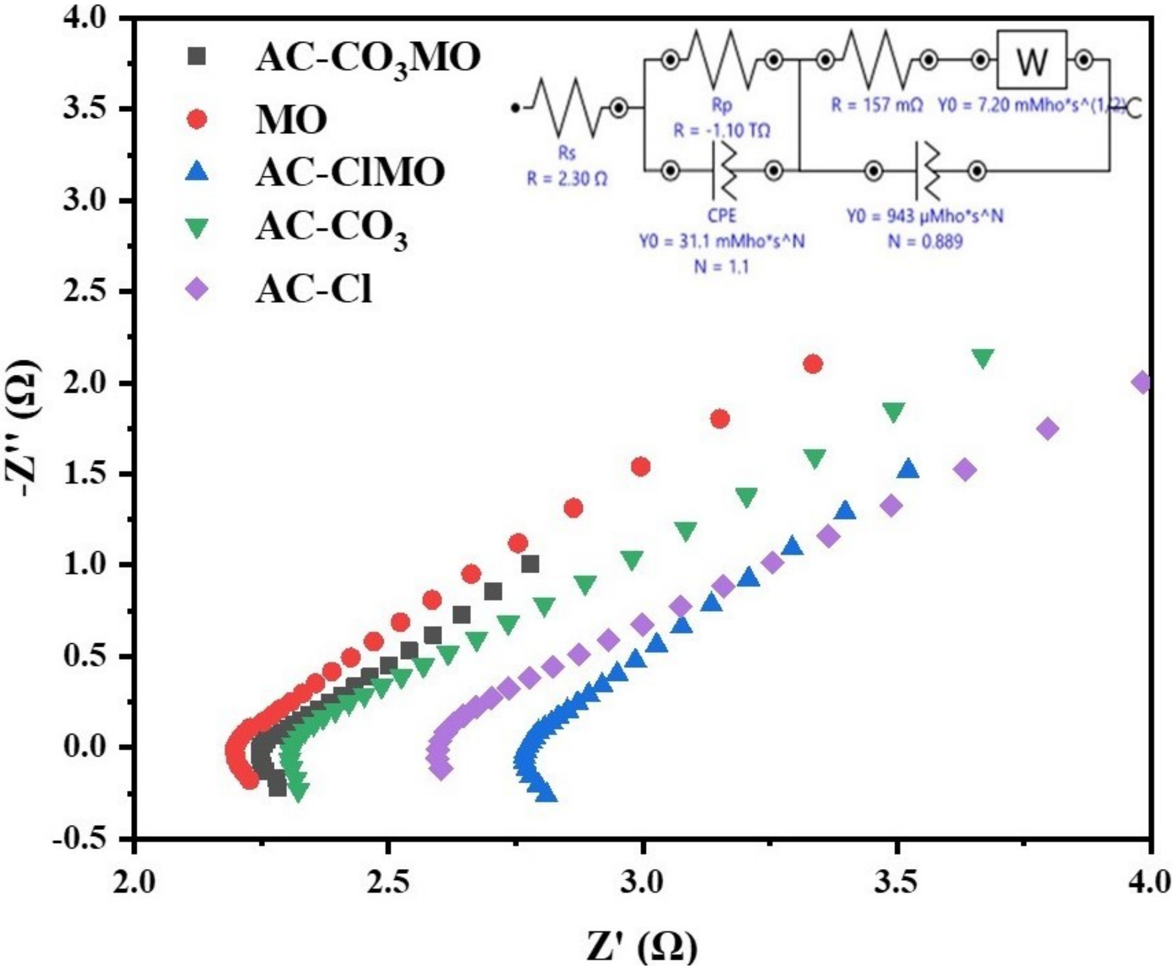

Figure S17: Magnified EIS Nyquist Plot (insight is equivalent circuit)

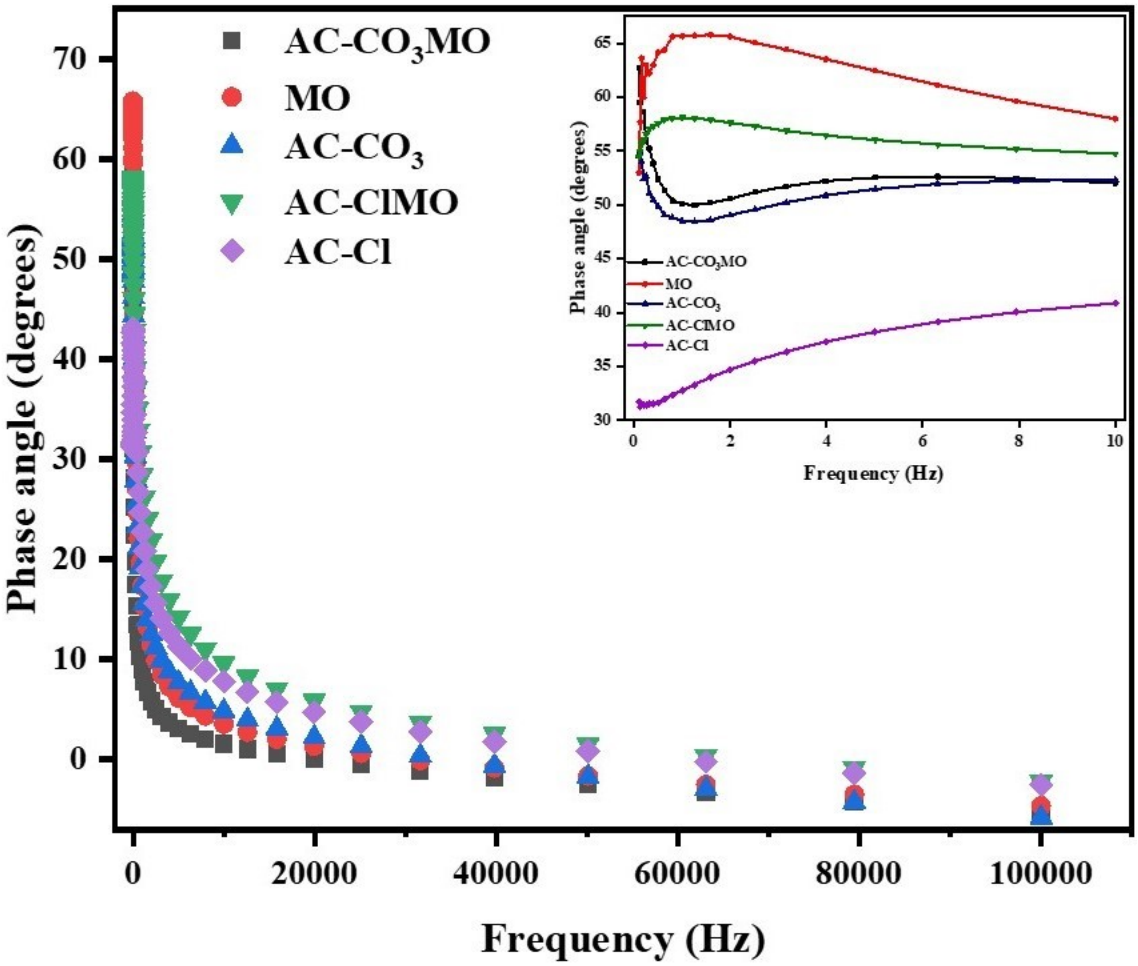

Figure S18: Bode Plot for Frequency vs Phase angle

Table S1: Ratio of $t_{discharging}/t_{charging}$ for different synthesized electrode materials

Electrode Materials	$t_{dsicharging}/t_{charging}$	S.D
AC-CO_3MO	2.86	2.86 ± 0.84
AC-CO_3	2.51	2.51 ± 0.84
AC-ClMO	1.66	1.66 ± 0.84
AC-Cl	1.22	1.22 ± 0.84
MO	0.88	0.88 ± 0.84

Table S2: Comparison of the capacitance of NDCs derived from different sources of biowaste

Carbon Precursor/Electroactive Materials	Chemical Activator	Nitrogen Source	Electrolyte	Capacitance	Retention/Cycles/ Current Density	Ref.
Soybean curd residue	Not used	Self-nitrogen	2(M) KOH	215 Fg^{-1} at 0.5 Ag^{-1}	90% / 5000 / 5Ag^{-1}	[1]
Shrimp shell	KOH	Self-nitrogen	6(M) KOH	348 Fg^{-1} at 0.05 Ag^{-1}	93.5% / 1000 / 1Ag^{-1}	[2]
Ascophyllum nodosum	KOH	N_2 source	1(M) KOH	207 Fg^{-1} at 0.5 Fg^{-1}	92.3% / 2500 / 5Ag^{-1}	[3]
AC/PANI/PVA	-	-	2(M) H_2SO_4	62.5 Fg^{-1} at 0.1 Ag^{-1}	84% / 3000 / 0.1 Ag^{-1}	[4]
Desmostachya bipinnata	KOH	-	6(M) KOH	218 $Fg-^{1}$ at 0.7 Ag^{-1}	85% / 5000 / 0.7 Ag^{-1}	[5]
Potato waste	$ZnCl_2$	Melamine	2(M) KOH	255 Fg^{-1} at 0.5 Ag^{-1}	93% / 5000 / 5 Ag^{-1}	[6]
Banana Fibres	$ZnCl_2$	-	1(M) Na_2SO_4	74 Fg^{-1} at 0.5 Ag^{-1}	88% / 500 / 0.5 Ag^{-1}	[7]
Borassus flabellifer Flower	H_3PO_4	-	1(M) KOH	238.2 Fg^{-1} at 1 Ag^{-1}	90% / 1000 / 1 Ag^{-1}	[8]
Waste Tea Leaves	KOH	-	2 (M) KOH	330 Fg^{-1} at 1 Ag^{-1}	92% / 2000 / 5 Ag^{-1}	[9]
Psidium guajava	$(NH_4)_2CO_3$	Urea	1(M) KOH	499 $mFcm^{-2}$ at 0.5 $mAcm^{-2}$	-	This work
Psidium guajava	NH_4Cl	Urea	1(M) KOH	223.7 $mFcm^{-2}$ at 0.5 $mAcm^{-2}$	-	This work
PNDC/$NiCo_2O_4$ (AC-CO_3 PNDC used)	**-**	**-**	**1(M) KOH**	**761.9 $mFcm^{-2}$at 0.5 $mAcm^{-2}$**	**66% / 800/ 10 $mAcm^{-2}$**	**This work**

References

[1] G. Ma et al., ***RSC Adv***, 2015, **5**, 83129–83138.

[2] F. Gao et al., ***J Mater Chem A Mater***, 2016, **4**, 7445–7452.

[3] K. Y. Perez-Salcedo et al., ***Journal of Porous Materials***, 2020, **27**, 959–969.

[4] A. Olad et al., ***Journal of Polymer Research***, 2016, **23**, 147,.

[5] G. K. Gupta et al., ***Nanoscale Res Lett***, 2021, **16**, 85.

[6] G. Ma *et al.*, ***Bioresour Technol***, 2015, **197**, 137–142.

[7] V. Subramanian et al., ***Journal of Physical Chemistry C***, 2007, **111**, 7527–7531.

[8] M. Sivachidambaram et al., ***New Journal of Chemistry***, 2017, **41**, 3939–3949.

[9] C. Peng et al., ***Electrochim Acta***, 2013, **87**, 401–408.